MIMO OVER-THE-HORIZON RADAR WAVEFORM DESIGN FOR TARGET DETECTION

Shuangling Wang, Qian He, Zishu He, and Rick S. Blum*[†]

EE Department, Univ. of Electron. Sci. and Tech. of China, Chengdu, Sichuan 611731 China
[†]ECE Department, Lehigh University, Bethlehem, PA 18015 USA

ABSTRACT

We study the waveform design problem for a multiple-input multiple-output over-the-horizon (MIMO-OTH) radar system faced with a combination of additive Gaussian noise and signal dependent clutter. Considering the operational frequency of the MIMO-OTH radar is generally limited to a certain frequency band due to propagation and implementation issues, the waveform transmitted at each antenna is constructed as a weighted sum of discrete prolate spheroidal (DPS) sequences which have good orthogonal and band-limited properties. Optimum waveforms (possibly nonorthogonal) are designed to maximize the target detection performance of the MIMO-OTH radar system with the constraint of fixed total transmitted energy. The performance of the proposed waveforms is analyzed.

Index Terms— Multiple-input multiple-output radar, over-the-horizon radar, signal detection, waveform design.

1. INTRODUCTION

Over-the-horizon (OTH) radar systems offer an efficient means for early warning by monitoring targets, such as low-flying aircraft, sea surface ship, and stealth aircraft, beyond the horizon [1–3]. Capitalizing on recent advances [4–11], the advantages of MIMO radar technology have recently been applied to OTH radar systems [12–16]. In this paper, an OTH radar system which uses MIMO radar techniques is called a MIMO-OTH radar system. Waveform design is a key issue in radar signal processing [17–20]. For MIMO-OTH radar systems, the authors in [13] use time-staggered and frequency-staggered linear frequency modulated continuous-wave (LFMCW) for MIMO-OTH radar systems. In [14], the authors consider fast-time orthogonal waveforms and propose to use slow-time MIMO methods, which can be easily implemented on legacy OTH radars. However, as far as we know, none of the existing works consider the design of optimum waveforms for MIMO-OTH radar systems. In this paper, we design waveforms by maximizing the detection performance of the MIMO-OTH radar systems, since the major responsibility of OTH radar system is the surveillance of targets over land and ocean.

To meet the strict frequency band limitations for OTH radar systems caused by the propagation and implementation issues such as the ionospheric reflection properties and external interference, we employ discrete prolate spheroidal (DPS) sequences [21] to form waveforms for our MIMO-OTH radar. DPS sequences are orthogonal. Considering DPS sequences with time duration $[0, N-1]$, Slepian pointed out that there are $2NW$ DPS sequences which are approximately band-limited to $[-W, W]$, where $W \leq 1/2$. Denote the k-th, $k = 1, ..., 2NW$ normalized DPS sequence time-limited to $[0, N]$ and band-limited to $[-W, W]$ by $v_k(n; N, W)$, $n = 0, ..., N-1$, then $\sum_{n=0}^{N-1} v_k(n; N, W) v_{k'}(n; N, W) = \delta_{k,k'}$, $k, k' = 1, ..., 2NW$, where $\delta_{k,k'}$ is the Kronecker delta function, which span a $2NW$-dimensional orthonormal space. In this paper, we construct each of the M transmit waveform as a weighted sum of the first $2NW$ DPS sequences, which reduces the waveform design problem to a $2NWM$-dimensional parameter optimization problem. Since the same set of orthogonal DPS sequences are used at every transmit antenna, the transmit waveforms can be made either orthogonal or nonorthogonal according to different combination of the weighing factors. We will show that the optimum waveforms that maximize the radar detection performance are sometimes nonorthogonal.

2. SIGNAL MODEL

Consider a MIMO-OTH radar equipped with M arbitrary spaced transmit antennas and L closely, and linearly, spaced receive antennas. The extension to arbitrary spaced receive antennas is straightforward. We design the waveform transmitted by the m-th transmit antenna at the n-th discrete-time sample as a weighted sum of the first $2NW$ DPS sequences as given by

$$s_m(n; \boldsymbol{d}_m) = \sum_{k=1}^{2NW} d_k^m v_k(n; N, W) = \boldsymbol{v}^T(n)\, \boldsymbol{d}_m, \tag{1}$$

where $\boldsymbol{v}(n) = [v_1(n; N, W), \cdots, v_{2NW}(n; N, W)]^T$ and the weighting vector $\boldsymbol{d}_m = [d_1^m, \cdots, d_{2NW}^m]^T$. Since the DPS sequences are orthogonal, the designed waveforms can be

*Correspondence: qianhe@uestc.edu.cn

This work was supported by the National Nature Science Foundation of China under Grants 61102142, 11076006, and 61032010, and by the National Science Foundation under Grant CCR-0829958.

either orthogonal or correlated depending on the combination of chosen weighting factors.

Assume that the signal propagation through the ionosphere is stable during the observation interval [22], so that the target return and clutter for each transmitter to receiver path can be regarded as the responses of two linear time-invariant (LTI) systems [23] with the transmitted signal as input. As transmissions with different incident angles may be reflected by different ionospheric layers, the target and clutter impulse response associated with different transmitted signals may not be the same. Define $h_t^m(n)$ and $h_c^m(n)$ as the target and clutter impulse responses associated with the signal transmitted from the m-th, $m = 1, \cdots, M$ transmit antenna. The combination of all M transmitted signals, after being scattered by the target/clutter and reflected by the ionosphere, arrives at the receiving array, where the signal received at the l-th receiver can be expressed as

$$r_l(n) = \left\{ \sum_{m=1}^{M} s_m(n; \boldsymbol{d}_m) \circledast \left[h_t^m(n) + h_c^m(n) \right] \right\} e^{-j(l-1)\phi_r} + z_l(n)$$

where $\circledast$ denotes the convolution operator, $z_l(n)$ is the noise at the l-th receiver, and ϕ_r represents the spatial phase difference between adjacent receivers. Stacking the N_R observations that contain the target return for all L receive antennas into a column vector, the $LN_R \times 1$ overall received signal vector can be expressed as

$$\begin{aligned} \boldsymbol{r} &= \left[r_1(0), \cdots, r_L(0), \cdots, r_1(N_R-1), \cdots, r_L(N_R-1) \right]^T \\ &= \boldsymbol{H}_t \boldsymbol{s} \otimes \boldsymbol{a}_r(\theta_r) + \boldsymbol{H}_c \boldsymbol{s} \otimes \boldsymbol{a}_r(\theta_r) + \boldsymbol{z} = \boldsymbol{x}_t + \boldsymbol{x}_c + \boldsymbol{z} \end{aligned} \qquad (2)$$

where $\otimes$ stands for the Kronecker product operator, $\boldsymbol{x}_t$ denotes the target return, $\boldsymbol{x}_c$ the clutter return, $\boldsymbol{a}_r(\theta_r) = [1, e^{-j\phi_r}, \cdots, e^{-j(L-1)\phi_r}]^T$, $\boldsymbol{s} = [\boldsymbol{s}^T(0), \cdots, \boldsymbol{s}^T(N-1)]^T$, and $\boldsymbol{s}(n) = [s_1(n; \boldsymbol{d}_1), \cdots, s_M(n; \boldsymbol{d}_M)]^T$. The $\boldsymbol{H}_t$ and $\boldsymbol{H}_c$ in (2) are $N_R \times MN$ matrices which have the form of

$$\boldsymbol{H}_\varepsilon = \begin{bmatrix} \boldsymbol{h}_\varepsilon^T(0) & \boldsymbol{h}_\varepsilon^T(-1) & \cdots & \boldsymbol{h}_\varepsilon^T(1-N) \\ \boldsymbol{h}_\varepsilon^T(1) & \boldsymbol{h}_\varepsilon^T(0) & \cdots & \boldsymbol{h}_\varepsilon^T(2-N) \\ \vdots & \vdots & \ddots & \vdots \\ \boldsymbol{h}_\varepsilon^T(N_R-1) & \boldsymbol{h}_\varepsilon^T(N_R-2) & \cdots & \boldsymbol{h}_\varepsilon^T(N_R-N) \end{bmatrix} \qquad (3)$$

where $\varepsilon = t$ or c, and $\boldsymbol{h}_\varepsilon(n) = [h_\varepsilon^1(n), \cdots, h_\varepsilon^M(n)]^T$. The noise term $\boldsymbol{z}$ is assumed to obey complex Gaussian distribution with mean zero and covariance matrix $\boldsymbol{R}_z = \mathbb{E}\{\boldsymbol{z}\boldsymbol{z}^H\}$, which is assumed to be independent of the target and clutter returns. Next we give some assumptions on the statistic of the target return $\boldsymbol{x}_t$ and clutter return $\boldsymbol{x}_c$.

Due to the limited allowable operating bandwidth, the range resolution cell size of the MIMO-OTH radar is usually larger than the target size. Thus one could employ a point target model so that the target impulse response is an impulse function. Considering that the ionospheric reflection may give rise to multipath propagation, it appears more appropriate to assume that the target impulse response has a finite time duration N_t. Assume $\boldsymbol{h}_t(n) \neq \boldsymbol{0}$ for n in $[0, N_t-1]$ and $\boldsymbol{h}_t(n) = \boldsymbol{0}$ otherwise. From (2) and (3), the statistics of the target return vector $\boldsymbol{x}_t$ is determined by the statistics of the $N_t M \times 1$ vector $\boldsymbol{h}_t = [\boldsymbol{h}_t^T(0), \cdots, \boldsymbol{h}_t^T(N_t-1)]^T$. Assume $\boldsymbol{h}_t$ is zero-mean complex Gaussian distributed with known covariance matrix $\boldsymbol{R}_{ht}$,which can be written as [19] $\boldsymbol{R}_{ht} = \mathbb{E}\{\boldsymbol{h}_t\boldsymbol{h}_t^H\} = \sum_{i=1}^{M_{low}} \lambda_i \boldsymbol{q}_i \boldsymbol{q}_i^H$ where $M_{low} \leq N_t M$ denotes the rank of $\boldsymbol{R}_{ht}$, λ_i represents the i-th largest eigenvalue of $\boldsymbol{R}_{ht}$, $\boldsymbol{q}_i \equiv [\boldsymbol{q}_i^T(0), \cdots, \boldsymbol{q}_i^T(N_t-1)]^T$ represents the corresponding orthonormal eigenvector, and $\boldsymbol{q}_i(n) \equiv [q_1^i(0), \cdots, q_M^i(N_t-1)]^T$. Thus $\boldsymbol{x}_t$ is zero-mean complex Gaussian distributed as it is described by a linear transformation of a complex zero-mean Gaussian vector $\boldsymbol{h}_t$. It can be shown that the covariance matrix of the target return can be expressed as

$$\boldsymbol{R}_t = \mathbb{E}\left\{\boldsymbol{x}_t\boldsymbol{x}_t^H\right\} = \sum_{i=1}^{M_{low}} \lambda_i \boldsymbol{y}_i^t \left(\boldsymbol{y}_i^t\right)^H = \boldsymbol{Y}_t \boldsymbol{\Sigma} \boldsymbol{Y}_t^H \qquad (4)$$

where $\boldsymbol{Y}_t = (\boldsymbol{y}_1^t, \cdots, \boldsymbol{y}_{M_{low}}^t)$, $\boldsymbol{\Sigma} = \mathrm{diag}\{\lambda_1, \cdots, \lambda_{M_{low}}\}$, $\boldsymbol{y}_i^t = \boldsymbol{Q}_i \boldsymbol{s} \otimes \boldsymbol{a}_r(\theta_r)$, and $\boldsymbol{Q}_i$ is an $N_R \times NM$ matrix constructed by $N_R \times N$ block matrices. The $\imath\jmath$-th ($\imath = 1, \cdots, N_R$ and $\jmath = 1, \cdots, N$) block of $\boldsymbol{Q}_i$ equals $\boldsymbol{q}_t^T(\imath - \jmath)$ for $0 \leq \imath - \jmath < N_t$ and $\boldsymbol{0}_{1\times M}$ otherwise.

From (2) and (3), the statistic of the clutter return vector $\boldsymbol{x}_c$ is determined by the statistics of a $(N_R + N - 1)M \times 1$ vector $\boldsymbol{h}_c = [\boldsymbol{h}_c^T(1-N), \cdots, \boldsymbol{h}_c^T(N_R-1)]^T$. Assume $\boldsymbol{h}_c$ is zero-mean complex Gaussian distributed with covariance matrix $\boldsymbol{R}_{h_c}$. Thus, $\boldsymbol{x}_c$ is also zero-mean complex Gaussian distributed, whose covariance matrix is given by

$$\boldsymbol{R}_c = \mathbb{E}\left\{\boldsymbol{x}_c\boldsymbol{x}_c^H\right\} = \boldsymbol{\xi} \otimes \left[\boldsymbol{a}_r(\theta_r)\,\boldsymbol{a}_r^H(\theta_r)\right], \qquad (5)$$

where $\boldsymbol{\xi} = \mathbb{E}\{(\boldsymbol{H}_c\boldsymbol{s}\boldsymbol{s}^H\boldsymbol{H}_c^H)\}$, the ij-th entry of which is

$$\xi_{ij} = \sum_{n,n'=0}^{N-1} \sum_{m,m'=1}^{M} s_m(n; \boldsymbol{d}_m)\, s_{m'}^*(n'; \boldsymbol{d}'_m)\, \boldsymbol{R}_{h_c,\imath\jmath} \qquad (6)$$

where $\imath = (N - n + i - 1)M + m$, $\jmath = (N - n' + j - 1)M + m'$ and the $\boldsymbol{R}_{h_c,\imath\jmath}$ denotes the ij-th entry of $\boldsymbol{R}_{h_c}$. From (5) and (6), it is easy to see that $\boldsymbol{R}_c$ is essentially determined by $\boldsymbol{R}_{h_c}$. Assume the covariance matrix of $\boldsymbol{h}_c$ satisfies $\boldsymbol{R}_{h_c} = \mathbb{E}\{\boldsymbol{h}_c\boldsymbol{h}_c^H\} = \boldsymbol{C}_T \otimes \boldsymbol{C}_S$, where $\boldsymbol{C}_S$ denotes the spatial correlation between clutter impulse responses corresponding to different transmissions for a fixed time index, and $\boldsymbol{C}_T$ denotes the temporal correlation between clutter impulse responses corresponding to different time delays for a fixed spatial index. Assume the ij-th element of the spatial correlation matrix $\boldsymbol{C}_S$ is $\boldsymbol{C}_{S,ij} = \sigma_S^2 \rho_S^{|i-j|}$, where σ_S^2 is a constant and $0 \leq \rho_S \leq 1$ denotes one-lag correlation coefficient. The temporal correlation matrix $\boldsymbol{C}_T$ is modeled as the covariance matrix of a time-varying autoregressive (TVAR) process [22], such that $\boldsymbol{C}_T^{-1} = \boldsymbol{A}^H \boldsymbol{E}_T^{-1} \boldsymbol{A}$ where $\boldsymbol{E}_T = \mathrm{diag}\{\sigma_T^2(1-N), \cdots, \sigma_T^2(N_R-1)\}$ is constructed from the time-varying variance of a white complex Gaussian process $\sigma_T^2(n)$, diag$\{\cdot\}$ denotes diagonal matrix, and $\boldsymbol{A}$ can be constructed [22] from an order-K TVAR coefficients $a_k(n), n = 1-N, \cdots, N_R - 1$.

3. DPS SEQUENCE-BASED WAVEFORM DESIGN FOR TARGET DETECTION

3.1. Detector Model and Performance Analysis

Based on the signal model in Section 2, we formulate the target detection problem as the following binary hypothesis testing problem

$$\begin{array}{lcl} \mathrm{H}_0 & : & \boldsymbol{r} = \boldsymbol{x}_c + \boldsymbol{z} \\ \mathrm{H}_1 & : & \boldsymbol{r} = \boldsymbol{x}_t + \boldsymbol{x}_c + \boldsymbol{z}. \end{array} \tag{7}$$

It can be shown that the test statistic of the optimum likelihood ratio test can be written as

$$\Lambda = \boldsymbol{r}^H \boldsymbol{C}_0^{-1} \tilde{\boldsymbol{Y}}_t \tilde{\boldsymbol{Y}}_t^H \boldsymbol{C}_0^{-1} \boldsymbol{r} = \boldsymbol{b}^H \boldsymbol{b} = \sum_{i=1}^{M_{low}} |b_i|^2 \tag{8}$$

where $\boldsymbol{C}_0 = \boldsymbol{R}_c + \boldsymbol{R}_z$ is covariance matrix of $\boldsymbol{r}$ under H_0 hypotheses, $\tilde{\boldsymbol{Y}}_t = \boldsymbol{Y}_t(\boldsymbol{Y}_t^H \boldsymbol{C}_0^{-1} \boldsymbol{Y}_t + \boldsymbol{\Sigma}^{-1})^{-1/2} \equiv (\tilde{\boldsymbol{y}}_1^t, \cdots, \tilde{\boldsymbol{y}}_{M_{low}}^t)$, and $b_i = (\tilde{\boldsymbol{y}}_i^t)^H \boldsymbol{C}_0^{-1} \boldsymbol{r}$. The b_i, which is a linear transformation of the zero-mean complex Gaussian random vector $\boldsymbol{r}$, also follows zero-mean Gaussian distribution.

In order to analyze the performance of the detector, next we calculate the distribution of test statistic under hypotheses H_0 and H_1. When hypothesis H_0 is true, the variance of b_i is $\sigma_{0i}^2 = (\tilde{\boldsymbol{y}}_i^t)^H \boldsymbol{C}_0^{-1} \tilde{\boldsymbol{y}}_i^t$ and the test statistic in (8) can be written as $\Lambda_0 = \sum_{i=1}^{M_{low}} \sigma_{0i}^2 B_{0i}/2$, where $B_{0i} = 2|b_i|^2/\sigma_{0i}^2$ obeys Chi-square distribution with two degrees of freedom. Thus, the test statistic Λ_0 is a weighted sum of correlated Chi-square random variables $B_{01}, B_{02}, \cdots, B_{0M_{low}}$, the distribution of which can be approximated by [24] $\Lambda_0 \sim \psi_0 \Gamma(\eta_0, 2)$, where $\Gamma(\tilde{\alpha}, \tilde{\beta})$ denotes gamma distribution with shape parameter $\tilde{\alpha}$ and scale parameter $\tilde{\beta}$, $\psi_0 = \{[\sum_{i=1}^{M_{low}} (\sigma_{0i}^2/2)]^2 + 2\sum_{i<j} \rho_{0ij} (\sigma_{0i}^2/2)(\sigma_{0j}^2/2)\}/[\sum_{i=1}^{M_{low}} (\sigma_{0i}^2/2)]$ with the constant ρ_{0ij} denoting the correlation coefficient of B_{0i} and B_{0j}, and $\eta_0 = \sum_{i=1}^{M_{low}} [\sigma_{0i}^2/(2\psi_0)]$. Thus, the false alarm probability P_{FA} can be obtained

$$P_{\mathrm{FA}} \equiv F_0(\gamma) = P(\Lambda_0 > \gamma) = \int_{\gamma/\psi_0}^{\infty} t^{\eta_0 - 1} \frac{e^{-\frac{t}{2}}}{2^{\eta_0} \Gamma(\eta_0)} dt. \tag{9}$$

Similarly, when hypothesis H_1 is true, the variance of b_i is $\sigma_{1i}^2 = \mathbb{E}\{|b_i|^2|\mathrm{H}_1\} = \sigma_{0i}^2 + |(\tilde{\boldsymbol{y}}_i^t)^H \boldsymbol{C}_0^{-1} \boldsymbol{Y}_t \boldsymbol{\Sigma}^{1/2}|$ and the test statistic can be written as $\Lambda_1 = \sum_{i=1}^{M_{low}} \sigma_{1i}^2 B_{1i}/2$ where $B_{1i} = 2|b_i|^2/\sigma_{1i}^2$. The distribution of Λ_1 can be approximated [24] by $\Lambda_1 \sim \psi_1 \Gamma(\eta_1, 2)$ where ψ_1 and η_1 can be obtained by replacing the σ_{0i}^2 and ρ_{0ij} in ψ_0 and η_0 with σ_{1i}^2 and ρ_{1ij}. Thus, the detection probability can be derived

$$P_{\mathrm{D}} \equiv F_1(\gamma) = P(\Lambda_1 > \gamma) = \int_{\gamma/\psi_1}^{\infty} t^{\eta_1 - 1} \frac{e^{-\frac{t}{2}}}{2^{\eta_1} \Gamma(\eta_1)} dt. \tag{10}$$

3.2. Waveform Design Based On DPS Sequences

Previously, we have analyzed the distribution of the test statistic under the null Λ_0 and alternative Λ_1 hypotheses. Assume that the total transmit energy is upper bounded by E_0. Our goal is to find the optimum waveforms which maximize the detection probability of a size-$\bar{\alpha}$ test under the Neyman-Pearson criterion. The optimization problem is give by

$$\max_{\boldsymbol{s}} F_1\left(F_0^{-1}(\bar{\alpha})\right) \quad s.t. \quad \|\boldsymbol{s}\|_2^2 \le E_0. \tag{11}$$

where $F_0^{-1}(\cdot)$ represents the inverse function of $F_0(\cdot)$. Note that the objective function in (11) is implicitly a function of the transmit waveforms $\boldsymbol{s}$. For simplicity and to get insight of the problem, next we consider a specific case where the covariance matrix of the target reflection coefficient vector has unit rank[1]. Assume that the target reflection coefficients $h_t^m(n)$ have identical random phase fluctuation ϕ for all m and n, such that $\boldsymbol{h}_t = \sqrt{\lambda_1} \boldsymbol{q}_1 e^{j\phi}$ where $\boldsymbol{q}_1$ is a deterministic vector. In this case, we have $M_{low} = 1$. The $\boldsymbol{R}_t$ in (4) becomes $\boldsymbol{R}_t = \lambda_1 \boldsymbol{y}_1^t (\boldsymbol{y}_1^t)^H$. Thus, the variances of b_1 under H_0 and H_1 hypotheses are $\sigma_{01}^2 = G(\boldsymbol{y}_1^t)^H \boldsymbol{C}_0^{-1} \boldsymbol{y}_1^t$ and $\sigma_{11}^2 = \sigma_{01}^2 + G|(\boldsymbol{y}_1^t)^H \boldsymbol{C}_0^{-1} \boldsymbol{y}_1^t|^2$ respectively, where $G = \lambda_1/[1 + \lambda_1 (\boldsymbol{y}_1^t)^H \boldsymbol{C}_0^{-1} \boldsymbol{y}_1^t]$. Applying M_{low}=1, we also have $\psi_0 = \sigma_{01}^2/2$, $\eta_0 = 1$, $\psi_1 = \sigma_{11}^2/2$ and $\eta_1 = 1$. Plugging them in (9) and (10) we get

$$P_{\mathrm{FA}} = F_0(\gamma) = \exp\left(-\gamma/\sigma_{01}^2\right) \tag{12}$$

and

$$P_{\mathrm{D}} = F_1(\gamma) = \exp\left(-\gamma/\sigma_{11}^2\right). \tag{13}$$

Substituting (12) and (13) into (11), the objective function turns out to be $F_1[F_0^{-1}(\bar{\alpha})] = \bar{\alpha}^{1/[1+(\boldsymbol{y}_1^t)^H \boldsymbol{C}_0^{-1} \boldsymbol{y}_1^t]}$. After manipulation, the optimization problem in (11) can be rewritten as

$$\begin{aligned} \max_{\boldsymbol{d}} \quad & \boldsymbol{d}^H \tilde{\boldsymbol{V}}^T \boldsymbol{Q}_1^H \boldsymbol{A}_R^H \boldsymbol{C}_0^{-1} \boldsymbol{A}_R \boldsymbol{Q}_1 \tilde{\boldsymbol{V}} \boldsymbol{d} \\ s.t. \quad & \boldsymbol{d}^H \boldsymbol{d} \le E_0 \end{aligned} \tag{14}$$

where $\boldsymbol{d} = [\boldsymbol{d}_1^T, \cdots, \boldsymbol{d}_M^T]^T$, $\tilde{\boldsymbol{V}} = [\boldsymbol{\Psi}^T(1), \cdots, \boldsymbol{\Psi}^T(N)]^T$, $\boldsymbol{\Psi}(i) = \mathrm{Diag}\{\boldsymbol{v}^T(i), \cdots, \boldsymbol{v}^T(i)\}$ is an $M \times 2NWM$ matrix, $\boldsymbol{A}_R = \mathrm{Diag}\{\boldsymbol{a}_r(\theta_r), \cdots, \boldsymbol{a}_r(\theta_r)\}$ is an $N_R L \times N_R$ matrix, and Diag$\{\cdot\}$ denotes block diagonal matrix. Due to the orthogonal property of the DPS sequences, we have $\tilde{\boldsymbol{V}}^T \tilde{\boldsymbol{V}} = \boldsymbol{I}$ such that the total transmit energy constraint becomes $\|\boldsymbol{s}\|_2^2 = \boldsymbol{s}^H \boldsymbol{s} = \boldsymbol{d}^H \tilde{\boldsymbol{V}}^T \tilde{\boldsymbol{V}} \boldsymbol{d} = \boldsymbol{d}^H \boldsymbol{d} \le E_0$. Next we solve (14) by an iterative method proposed by Pillai et al in [25] to obtain the optimum waveforms parameters $\boldsymbol{d}^{\mathrm{opt}}$. Then, the optimum DPS sequence-based waveforms $s_1^{\mathrm{opt}}(n), \cdots, s_4^{\mathrm{opt}}(n)$ can be obtained by plugging $\boldsymbol{d}^{\mathrm{opt}}$ into (1).

4. NUMERICAL RESULTS

Consider a MIMO-OTH radar equipped with $L = 2$ receivers and M transmitters. The total transmit energy is $E_0 = 4$. Suppose that due to propagation and implementation issues, the

[1] Analysis of the general case will be presented in future publications.

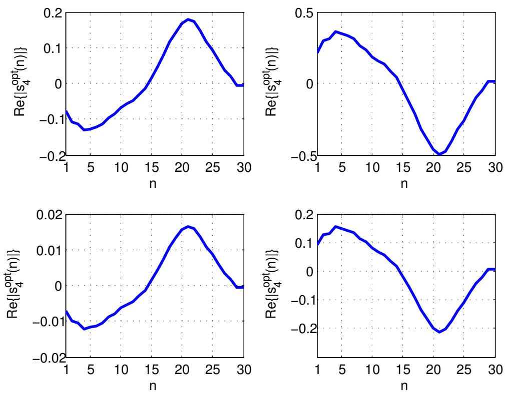

Fig. 1. Real parts of the optimum waveforms transmitted from four antennas.

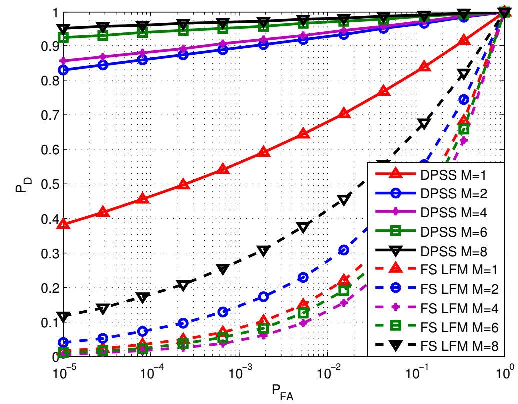

Fig. 2. ROCs for the DPS sequence-based waveforms and FS LFM signals for a different number of transmitters M.

allowable operational frequency is centered at $f_0 = 10$MHz with a bandwidth of $B = 1.5$KHz, so the transmitted waveforms are frequency limited to $[f_0 - B/2, f_0 + B/2]$. Assume the transmit signals have pulse width $T = 16$ms and the sampling frequency is $f_s = 1.875$KHz, resulting in the number of samples $N = Tf_s = 30$ and the relative bandwidth $W = B/(2f_s) = 0.4$. Suppose a target, if present, is located at $\theta_r = 30°$. Assume $N_t = 8$ and $N_R = 37$. The clutter covariance matrix is computed using (5) and the noise is assumed to be temporally colored and spatially white (see [26] for detail). Given these parameters, we employ Pillai's method [25] to solve for the optimum $\boldsymbol{d}$ in (14), and the optimum value $\boldsymbol{d}^{\text{opt}}$ is plugged into (1) to compute the optimum waveforms. When $M = 4$, assume $\boldsymbol{q}_1(n) = [0.65, -1.77, 0.06, -0.76]$ for n in $[0, N_t - 1]$. The real parts of the optimum waveforms $s_m^{opt}(n)$ are plotted in Fig. 1. We find that in this example the optimum waveforms are non-orthogonal. In other words, orthogonal waveforms are not always the best solution for MIMO-OTH radar detection.

Next, we look at the detection performance of the waveforms designed by the proposed method. We present the effects of changing the number of transmit antennas and compare the detection performance of the designed waveforms with that obtained from frequency spread (FS) LFM signals, which are commonly used in traditional OTH radar systems. The m-th FS LFM signal is assumed to be $s_m(t) = \sqrt{E_0/(MN)}rect(t/T)e^{j2\pi[(f_0-B/2)t+\mu t^2/2+(m-1)\Delta f t]}, m = 1, \cdots, M$, where Δf is the frequency offset , $\mu = B_u/T$, and B_u is the bandwidth of u_m for any m. Considering the frequency requirement of the MIMO-OTH radar as stated previously, we let $\Delta f = 1/T$ and $B_u = B - (M - 1)/T$. For several different values of M, we plot the receiver operating characteristics (ROCs) for the optimum DPS sequence-based waveforms and FS LFM signals in Fig. 2. It is seen that for any given M, the ROC curves of the optimum DPS sequence-based waveforms are uniformly higher than that of the FS LFM signals, indicating the superiority of our designed signals when compared with the signals often used in traditional OTH radar systems. We find that for the DPS sequence-based waveforms, the detection performance is improved when the number of transmit antennas is increased. While for a MIMO-OTH radar employing FS LFM signals, the detection performance is not necessarily improved with the increase of transmit antennas. Intuitively, for the FS LFM signals, increasing M will increase the beamforming gain which can enhance the detection performance. However, since the total bandwidth B of the MIMO-OTH radar is limited and the frequency offset Δf is fixed to $1/T$ to attain orthogonality, when we continue adding transmit antennas, the bandwidth B_u of each signals will be reduced, leading to a performance degradation. For the DPS sequence-based waveforms, the detection performance will not be degraded with the increase of transmit antennas since the orthogonality of the basis functions does not have to be separate in frequency, and further the waveforms are not restricted to be orthogonal.

5. CONCLUSIONS

This paper considered the waveforms constructed by a weighted sum of DPS sequences with sample number N and relative bandwidth W which are determined by the MIMO-OTH radar system parameters. We designed the waveforms by maximizing the detection performance under the constraint of the bandwidth and total energy restrictions. We showed that the waveform design problem can be reduced to the optimization of the $2NWM$ weighting factors. The optimum DPS sequence-based waveforms turn out to be nonorthogonal, which implies that orthogonal signals are not always the best. We showed that the designed DPS sequence-based waveforms have superior detection performance than the FS LFM signals. When the number of transmit antennas is increased, the detection performance of the DPS sequence-based waveforms is improved, while it is not always the case for the FS LFM signals possibly due to the limited bandwidth.

References

[1] B.T. Root, "HF-over-the-horizon radar ship detection with short dwells using clutter cancellation," *Radio Sci.*, vol. 33, no. 4, pp. 1095–1111, 1998.

[2] C.J. Coleman, "A model of HF sky wave radar clutter," *Radio Science*, vol. 31, no. 4, pp. 869–875, 1996.

[3] J. Barnum, "Ship detection with high-resolution HF skywave radar," *IEEE Journal of Oceanic Engineering*, vol. 11, no. 2, pp. 196–209, 1986.

[4] A. Aubry, M. Lops, A.M. Tulino, and L. Venturino, "On MIMO detection under non-Gaussian target scattering," *IEEE Transactions on Information Theory*, vol. 56, no. 11, pp. 5822–5838, 2010.

[5] Y. Yu, A.P. Petropulu, and H.V. Poor, "Power allocation for CS-based colocated MIMO radar system," *IEEE Sensor Array and Multichannel Signal Processing Workshop*, pp. 217–220, 2012.

[6] X. Song, P. Willett, S. Zhou, and P.B. Luh, "The MIMO radar and jammer games," *IEEE Transactions on Signal Processing*, vol. 60, no. 2, pp. 687–699, 2012.

[7] T. Aittomaki and V. Koivunen, "Performance of MIMO radar with angular diversity under Swerling scattering models," *IEEE Journal of Selected Topics in Signal Processing*, vol. 4, no. 1, pp. 101–114, 2010.

[8] A.D. Maio, M. Lops, and L. Ventura, "Diversity-integration trade-off in MIMO detection," *IEEE Transacations on Signal Processing*, vol. 56, no. 10, pp. 4151–4161, 2008.

[9] J. Li and P. Stoica, *MIMO Radar Signal Processing*, Wiley, New York, 2009.

[10] Q. He and R.S. Blum, "Diversity gain for MIMO Neyman-Pearson signal detection," *IEEE Transacations on Signal Processing*, vol. 59, no. 3, pp. 869–881, 2011.

[11] Q. He, R.S. Blum, H. Godrich, and A.M. Haimovich, "Target velocity estimation and antenna placement for MIMO radar with widely separated antennas," *IEEE Journal of Selected Topics in Signal Processing*, vol. 4, no. 1, pp. 79–100, 2010.

[12] Y.I. Abramovich, G.J. Frazer, and B.A. Johnson, "Noncausal adaptive spatial clutter mitigation in monostatic MIMO radar: Fundamental limitations," *IEEE Journal of Selected Topics in Signal Processing*, vol. 4, no. 1, pp. 40–54, 2010.

[13] G.J. Frazer, Y.I. Abramovich, and B.A. Johnson, "Multiple-input multiple-output over-the-horizon radar: experimental results," *IET Radar, Sonar and Navigation*, vol. 3, no. 4, pp. 290–303, 2009.

[14] J. Krolik, V. Mecca, O. Kazanci, and I. Bilik, "Multipath spread-Doppler clutter mitigation for over-the-horizon radar," in *Radar Conference*. IEEE, 2008, pp. 1–5.

[15] R.J. Riddolls, M. Ravan, and R.S. Adve, "Canadian HF over-the-horizon radar experiments using MIMO techniques to control auroral clutter," in *Radar Conference*. IEEE, 2010, pp. 718–723.

[16] X. Li, Q. He, and Z. He, "Detection performance of MIMO-OTH radar: Advantages of multipath ionoshperic propagation," in *Proceedings of 2012 International Symposium on Advanced Computing and Communications*, 2012.

[17] S. Kay, "Optimal signal design for detection of Gaussian point targets in stationary Gaussian clutter / reverberation," *IEEE Journal of Selected Topics in Signal Processing*, vol. 1, no. 1, pp. 31–41, 2007.

[18] F. Yin, C. Debes, and A.M. Zoubir, "Parametric waveform design using discrete prolate spheroidal sequences for enhanced detection of extended targets," *IEEE Transactions on Signal Processing*, 2012.

[19] B. Friedlander, "waveform design for MIMO radars," *IEEE Transactions on Aerospace and Electronic Systems*, vol. 43, no. 5, pp. 1227–1238, 2007.

[20] Y. Yang and R.S. Blum, "MIMO radar waveform design based on mutual information and minimum mean-square error estimation," *IEEE Transactions on Aerospace and Electronic Systems*, vol. 43, pp. 330–343, 2007.

[21] D. Slepian and H.O. Pollak, "Prolate spheroidal wave functions, Fourier analysis and uncertainly. V. the discrete case," *Bell Systems Tech. J.*, vol. 57, pp. 1371–1430, 1978.

[22] D. Ramakrishnan and J. Krolik, "Adaptive radar detection in doubly nonstationary autoregressive Doppler spread clutter," *IEEE Transactions on Aerospace and Electronic Systems*, vol. 45, no. 2, pp. 484–501, 2009.

[23] M.R. Bell, "Information theory and radar waveform design," *IEEE Transactions on Information Theory*, vol. 39, no. 5, pp. 1578–1597, 1993.

[24] L. Chuang and Y.S. Shih, "Approximate distributions of weighted sum of correlated Chi-square random variables," *Journal of Statistical Planning and Inference*, vol. 142, no. 2, pp. 457–472, 2012.

[25] S.U. Pillai, H.S. Oh, D.C. Youla, and J.R. Guerci, "Optimal transmit-receiver design in the presence of signal-dependent interference and channel noise," *IEEE Transactions on Information Theory*, vol. 46, no. 2, pp. 577–584, 2000.

[26] S. Wang, Q. He, Z. He, and R.S. Blum, "DPS sequence-based waveform design for MIMO over-the-horizon radar detection," *submitted to IEEE Transactions on Aerospace and Electronic Systems*.